ELSEVIER

Polymer 42 (2001) 9791–9799

polymer

www.elsevier.com/locate/polymer

Influence of comonomer content and short branch length on the physical properties of metallocene propylene copolymers

Humberto Lovisi[a], Maria Inês B. Tavares[a], Naira M. da Silva[b], Sônia M.C. de Menezes[b], Luiz Claudio de Santa Maria[c], Fernanda M.B. Coutinho[a,c,*]

[a]Instituto de Macromoléculas Professora Eloisa Mano, Universidade Fed do Rio de Janeiro, P.O. Box 68525, Rio de Janeiro, CEP 21945-970, Brazil
[b]Petrobras/Cenpes/Diquim, CEP 21949-900, Rio de Janeiro, Brazil
[c]Grupo de Polímeros, Instituto de Química, UERJ, CEP 20559-900, Rio de Janeiro, Brazil

Received 5 February 2001; received in revised form 2 July 2001; accepted 5 July 2001

Abstract

In this work, new copolymers of propylene/1-hexene (PHC) and propylene/1-octene (POC) were synthesized by using a highly isospecific metallocene catalyst system based on *rac*-$Me_2Si(2\text{-ethyl,4-phenyl,1-indenyl})_2ZrCl_2$, in the homogeneous and heterogeneous forms, activated by methylaluminoxane (MAO). An investigation about the copolymerization of propylene with 1-hexene and 1-octene employing this catalyst system illustrates the potential for the tailoring of propylene/higher α-olefin copolymers with controlled thermal and mechanical properties by varying the comonomer concentration in the polymerization feed. Both catalyst systems showed high activity and produced random copolymers with very low or no detectable crystallinity. It was observed that properties such as enthalpy of crystallization (ΔH_c), crystallization temperature (T_c), melting temperature (T_m), glass transition temperature (T_g), storage modulus (E') and density decreased in a linear pattern with increasing comonomer content in the copolymer. That might allow to suggest differential scanning calorimetry (DSC) and dynamic thermal mechanical analysis (DMTA) as fast and low cost analytical methods to determine comonomer content in propylene copolymers, in the range of concentration studied, as a less expensive alternative to Solution State Carbon 13 Nuclear Magnetic Resonance (^{13}C NMR). The influence of the short chain branch length was also investigated and it was observed that, compared to 1-hexene, much less 1-octene was necessary to disrupt the crystalline structure and impart rubbery behavior to the copolymers. Solid state ^{13}C NMR analysis presented excellent correlation with the results obtained with DMTA. A lowering of $T_{1\rho}^{H}$ values was observed for copolymers with higher comonomer content and longer alkyl branch, which parallels the decline of storage modulus (E') and glass transition temperature (T_g), indicating an increase in materials' flexibility. © 2001 Elsevier Science Ltd. All rights reserved.

Keywords: Metallocene catalysts; Propylene/1-hexene copolymers; Propylene/1-octene copolymers

1. Introduction

Metallocene catalysts have been very successful in replacing Ziegler–Natta catalysts in the polyethylene industry. However, the same growth has not yet been experienced by polypropylene producers. That is partly due to the fact that only recently stereorigid bridged substituted bisindenyl zirconocenes were developed [1–5].

The advent of stereorigid dimethylsilylene-brigded bisindenylzirconocenes with substituents in the 2- and 4-positions led to highly active catalysts for propylene polymerization. These catalysts are capable of producing high molecular weight isotactic polypropylene with narrow molecular weight distribution and high melting temperatures [1–5]. Moreover, these metallocenes allow a much higher degree of α-olefin incorporation than could ever be achieved with conventional Ziegler–Natta catalysts. Generally, copolymerizations initiated by ordinary Ziegler–Natta catalysts produce copolymers with a wide comonomer distribution due to the heterogeneity of active species, whereas metallocene catalysts are able to produce copolymers with uniform comonomer distribution and low xylene extractables [5]. Thus, a new family of propylene copolymers with properties still not available within the range of commercial products can now be produced with very promising perspectives.

Metallocene ethylene/higher α-olefins copolymers are already one of the most important commercial products in the polyolefins market and have been widely studied in recent years [6–11]. However, not much has been published on propylene/higher α-olefin copolymers [12–25].

---

* Corresponding author. Tel.: +55-21-562-7210; fax: +55-21-270-1317.
E-mail address: fern@ima.ufrj.br (F.M.B. Coutinho).

0032-3861/01/$ - see front matter
PII: S0032-3861(01)00528-6

In the present study, a series of propylene/higher α-olefin copolymerizations were performed using a highly active and isospecific metallocene catalyst, i.e. *rac*-Me_2Si(2-ethyl,4-phenyl,1-indenyl)$_2ZrCl_2$. As far as we are aware of, there are only a few reports on propylene copolymerization with higher α-olefins [13–25]. None of them, however, regards the use of this highly isospecific catalyst. Furthermore, there is scarce information on the physical properties of these materials [13,14,21,24]. This paper discusses the structure–property relationships of propylene/1-hexene (PHC) and propylene/1-octene (POC) copolymers based on their thermal and solid state ^{13}C NMR characterization. Also, the influence of comonomer content and the length of the alkyl branch on the physical properties of metallocene propylene/higher α-olefin copolymers has been investigated.

Differential Scanning Calorimetry (DSC), Dynamic Mechanical Thermal Analysis (DMTA) and solid state ^{13}C NMR were used in this work in order to evaluate these new materials and to infer about their possible applications.

2. Experimental

2.1. Materials

Polymerization grade propylene was supplied by Polibrasil and further purified by passing through 4 Å molecular sieves and copper catalyst columns in order to remove residual water and oxygen. Commercial toluene was furnished by Shell and treated with 4 Å molecular sieves, refluxed with sodium and distilled right before use. 1-Hexene, 97 wt% purity and 1-octene, 98 wt% purity, were acquired from Sigma–Aldrich and further purified by refluxing with calcium hydride or sodium, respectively, and distilled prior to use. Metallocene catalyst [*rac*-Me_2Si(2-ethyl,4-phenyl,1-indenyl)$_2ZrCl_2$], with a purity higher than 98 wt% of the racemic isomer, was donated by Boulder Scientific and used as received. Methylaluminoxane (MAO) in toluene (10% w/v) was kindly donated by Witco GmbH and used as received. Microspheroidal silica MS 3070, with a surface area of 700 m^2/g, particle diameter of 90 μ and pore volume of 1.8 ml/g was kindly provided by PQ Corporation.

2.2. Catalyst heterogenization

Silica (2.0 g) was dried and partially dehydroxylated at 400°C for 5 h, under nitrogen flow, then treated with 34.5 mmol MAO in 70 ml toluene under nitrogen atmosphere, for 12 h. The MAO treated silica was filtered and washed with toluene (50 ml) for five times to remove excess MAO. A metallocene solution (0.1 mmol/50 ml toluene) was added to the MAO treated silica and stirred for 3 h at room temperature. The catalyst was filtered and washed with toluene, dried under vacuum and analysed by Inductively Coupled Plasma Spectroscopy (ICP) to determine Al and Zr contents. The heterogeneous catalyst used in this work has a Zr content of 0.15 wt% and Al = 11.0 wt%.

2.3. Polymerization

PHC and POC were produced batchwise in a Büchi pressure reactor using 1.0 μmol of the catalyst *rac*-Me_2Si(2-ethyl,4-phenyl,1-indenyl)$_2ZrCl_2$, either in the homogeneous or heterogeneous forms. MAO (5.1 mmol) was used as cocatalyst for homogeneous reactions (PP1, PP2, all PHC and POC17) (see Table 1). Heterogeneous catalysts were prepared according to the above procedure and used for reactions (all POC reactions but POC17) (Table 1). Additional external MAO (500 μmol) was added in heterogeneous reactions. Toluene (100 ml) was employed as diluent. All reactions were carried out at 55°C and 2 bar (gauge), except for PP1, which was obtained at 40°C. The concentration of propylene in toluene was determined experimentally according to a procedure described elsewhere [26]. The concentration of comonomer in the feed was varied from 0.0 up to 46 mol% so as to produce a wide range of copolymers.

2.4. Characterization

Polymer samples were characterized by ^{13}C NMR, SEC, DSC and DMTA.

2.4.1. Size exclusion chromatography (SEC)

Molecular weight and molecular weight distribution of the copolymers were determined in a Waters 150CV-Plus chromatograph equipped with a differential refractive index detector and a set of three columns, Styragel HT3, HT5 and HT6. Columns were calibrated using monodisperse polystyrene (PS) standards. Molecular weights (M_w) in Table 1 are PS equivalents. Analysis were performed at 135°C using 1,2,4-trichlorobenzene as solvent at 1.0 ml/min. Samples were dissolved in 1,2,4-trichlorobenzene in a concentration of 0.2% w/v and protected with Irganox 1010 (0.002% w/v) in order to prevent degradation during analysis.

2.4.2. Differential scanning calorimetry (DSC)

DSC measurements were performed in a Perkin–Elmer DSC-7 instrument, previously calibrated with indium metal. Samples were heated from 60 to 180°C at a heating rate of 10°C/min and cooled down to 60°C at the same rate. Melting temperatures were determined from the second heating curve.

2.4.3. Dynamic mechanical thermal analysis (DMTA)

Dynamic mechanical experiments were conducted in a Polymer Laboratories Dynamic Mechanical Thermal Analyser Mk III Instrument in the bending mode. Measurements were carried out at 1 Hz and temperature ranged from −80°C to the next melting point of each copolymer. The heating rate was 2°C/min. Samples were compression molded as rectangular plaques of 2 mm × 10 mm × 20 mm (thickness × width × length) at different temperatures, depending on comonomer content.

Table 1
Physical properties of metallocene propylene homopolymers and copolymers

Sample[a,b,c]	Type of comonomer	Comonomer (mol%)	M_w[d,e] (kg/gmol)	T_g (°C)	T_c (°C)	T_m (°C)	Density	Tan δ	$T_{1\rho}^H$ (ms)[f]
PP1	None	0.0	400	12.0	114	160	0.916	0.0593	26.8
PP2	None	0.0	90	–	114	155	–	–	–
PHC7	Hexene	6.6	70	10.0	103	148	0.907	0.0803	21.4
PHC10	Hexene	9.9	60	5.7	94	142	0.905	0.0957	17.6
PHC16	Hexene	15.7	60	0.5	80	139	0.895	0.1887	16.7
PHC21	Hexene	20.7	50	−8.3	[g]	[g]	0.886	0.3150	15.2
POC2	Octene	2.0	245	14.8	96	143	0.904	0.0846	–
POC4	Octene	4.0	85	10.0	87	125	–	0.1593	23.4
POC5	Octene	5.3	165	6.0	69	113	0.893	0.1965	–
POC7	Octene	7.0	140	6.3	[g]	[g]	0.887	0.2669	10.4
POC8	Octene	7.8	160	6.0	[g]	[g]	0.886	0.2754	–
POC9	Octene	9.4	120	−4.6	[g]	[g]	–	0.3715	–
POC17	Octene	16.5	105	−7.0	[g]	[g]	0.874	0.5745	7.7
POC20	Octene	20.0	200	−17.4	[g]	[g]	0.858	–	–

[a] Number in copolymers sample codes indicate the comonomer content (mol%).
[b] Al/Zr = 5100 for all homogeneous reactions (PP1, PP2, all PHC and POC17).
[c] Al/Zr = 500 for the heterogeneous reactions (all POC except POC17).
[d] All reactions were carried out at $P = 2$ bar and $T = 55$°C, except for sample PP1 ($T = 40$°C).
[e] MWD ≅ 2.0 for all polymers. Relative M_w values compared to monodisperse PS standards.
[f] Average values for $T_{1\rho}^H$ based on Table 2.
[g] No crystallinity was detected by DSC.

2.4.4. Density

The densities of the copolymers were determined according to the procedure described in the ASTM D792 [27]. Compression molded rectangular plaques (2 mm × 10 mm × 20 mm) were used for density measurement.

2.4.5. Carbon 13 nuclear magnetic resonance

^{13}C NMR spectra of samples were recorded in a Varian MERCURY 300 spectrometer operating at 74.5 MHz, on a 40% polymer solution in 1,2 dichlorobenzene at 90°C. Benzene-d6 was used for the internal lock in a 10 mm NMR probe. Experimental parameters are listed as follows: acquisition time, 1.815 s; relaxation delay, 15.0 s; pulse angle, 90° (21.5 μs); 64 K data points; 20 K transients. Proton decoupling was achieved with the WALTZ 16 sequence. Comonomer content in the propylene copolymers was calculated according to the method proposed by Cheng [28] and are presented in Table 1.

2.4.6. Solid state carbon 13 nuclear magnetic resonance

Measurements of the proton spin-lattice relaxation in the rotating frame ($T_{1\rho}^H$) were performed in a Varian INOVA 300 NMR spectrometer equipped with a cross-polarization-magic angle spinning (CPMAS) probe operating at 74.5 MHz (7.1 T). A pulse angle of 90° (5.5 μs) and a 1 s pulse interval was used. All measurements were made at room temperature. A proton RF field of 45 kHz and a contact time of 2 ms were employed throughout the experiments. The spinning speed at the magic angle was about 4 kHz. The pulse sequence used in the experiments was the Delayed Contact Time [29]. In this pulse sequence, the contact time is fixed and the spin locking time is varied. Acquisition is made after the contact while the proton decoupler is on. This method gives equivalent results to the conventional variable high power decoupler contact time experiment in measuring $T_{1\rho}^H$ of crystalline samples and is especially indicated for elastomeric and amorphous systems. For each sample, 10–12 data points were collected and a 20 Hz line broadening applied. All the acquired data look like the data shown in Fig. 11. All the relaxation data were fitted with a spreadsheet program on a personal computer, assuming a single-exponential (first order) decay.

3. Results and discussion

Some previous considerations regarding the copolymers preparation are required before discussing their physical properties listed in Table 1. First, the metallocene catalyst used in this work, *rac*-Me_2Si(2-ethyl,4-phenyl,1-indenyl)$_2$-$ZrCl_2$, is highly isospecific. ^{13}C NMR characterization of the samples have shown that the formation of stereo and regio defects, for the polymerization conditions used herein, are insignificant if compared to comonomer defects. Besides, according to the work of Busico et al. [30] and our own experimental data [31], it is known that the formation of stereo and regio defects in propylene polymerization catalyzed by isospecific metallocenes are quite dependent on polymerization temperature and pressure. Thus, since all reactions were carried out at the same pressure (2 bar) and temperature (55°C) (except for PP1, where $T = 40$°C), all observed

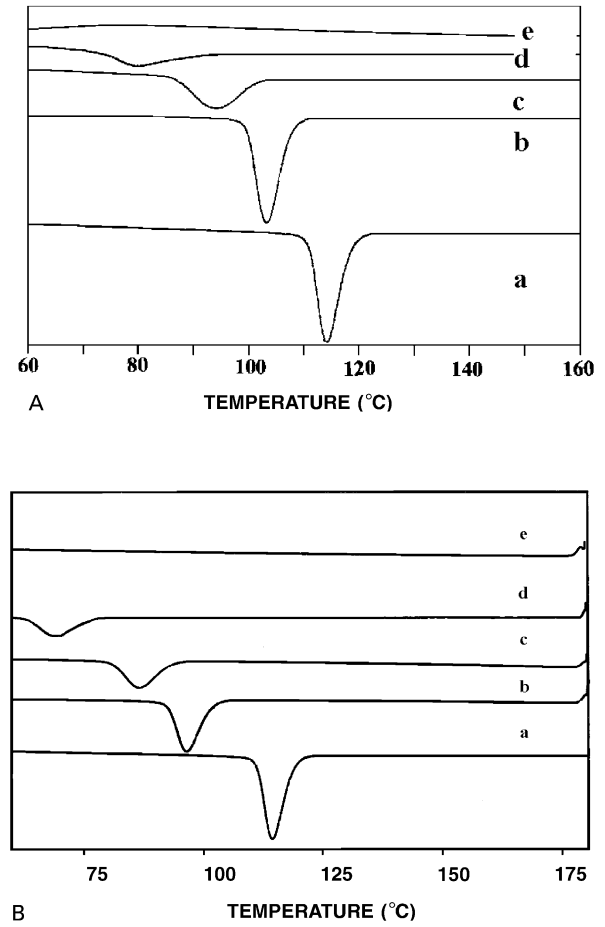

Fig. 1. (A) DSC crystallization curves for copolymers with increasing amounts of 1-hexene: (a) [1-hexene] = 0.0, (b) 6.6, (c) 9.9, (d) 15.7, (e) 20.7 mol%. (B) DSC crystallization curves for copolymers with increasing amounts of 1-octene: (a) [1-octene] = 0.0, (b) 2.0, (c) 4.0, (d) 5.3, (e) 7.0 mol%.

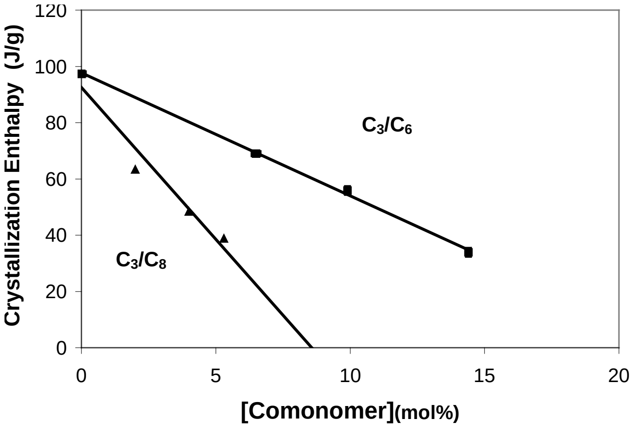

Fig. 2. Dependence of crystallization enthalpy on the comonomer content in the copolymer: (■) propylene/1-hexene: (▲) propylene/1-octene.

changes in physical properties should only be attributed to the defects caused by comonomer incorporation into the copolymer chain. Second, differences in molecular weight were considered not to significantly affect the copolymers physical properties. All M_ws are higher than 50,000 g/gmol and the effect of end groups in chain mobility was considered to be negligible in comparison to the greater influence of comonomer incorporation. Differences between homogeneous and heterogeneous catalysis will be addressed in a separate paper [31]. Nevertheless, the main difference in properties observed for these two set of copolymers was an increase in molecular weight due to the heterogenization of the catalyst.

Third, copolymers are assumed to have a random comonomer distribution along the chain. It was observed during the kinetic studies [31] that, for the high comonomer concentrations in the reactor feed used in this work ([comonomer] = 6–46 mol%), the kinetics of copolymerization was strongly inhibited. Copolymerizations were stopped after 30 min of reaction, when a significant amount of comonomer had not yet reacted. So, the product of reactivity ratios for copolymers presented in Table 1 ($r_p r_c$) is approximately one, as determined by ^{13}C NMR, which means a random distribution of the comonomer has been achieved. A more detailed discussion on the results of the copolymerization kinetic studies will be presented in a forthcoming paper [31]. All copolymer samples presented a narrow and single crystallization peak (Fig. 1). All crystallization temperatures were lower than that of pure homopolymer and no transition at the homopolymer region was observed in the copolymers crystallization curves. No broadening of the molecular weight distribution was detected (MWD ≈ 2.0), which would be expected in the case of a mixture of homopolymer and copolymers with different degrees of ramification and thus, different hydrodynamic volumes. So, all these evidences make it quite reasonable to assume these copolymers to have a homogeneous comonomer distribution.

Table 1 presents a list of all copolymers that were produced and their main properties. It can be immediately observed the large range of molecular weights and comonomer contents obtained with this versatile catalyst system, proving its capability for tailoring olefin copolymers with controlled thermal and mechanical properties.

Fig. 1 shows the crystallization curves for propylene homopolymer and PHC (Fig. 1a) and for POC (Fig. 1b) with different comonomer contents. As the comonomer content increases, the crystallization temperature and the enthalpy of crystallization drop to lower values. Actually, a linear relationship exists between comonomer content and crystallization temperature (T_c) or enthalpy of crystallization (ΔH_c) for both types of copolymers (Figs. 2 and 3). When the concentration of 1-hexene reaches 21 mol%, no more crystallization can be detected and it seems the material is amorphous (Fig. 1a). In fact, increasing amounts of higher α-olefin incorporated into the copolymer, gradually disrupt the crystalline structure, since the short branches will impart defects to the

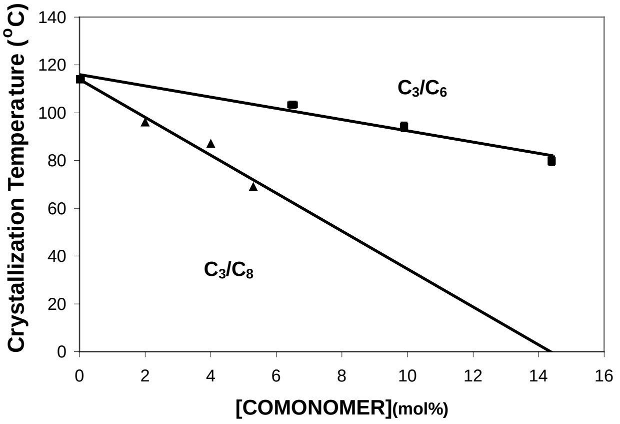

Fig. 3. Influence of comonomer content in the copolymer on the crystallization temperature: (■) propylene/1-hexene; (▲) propylene/1-octene.

polymer chain, creating obstacles for the organization of the crystalline region.

This effect becomes more intense for longer branches, so in the case of POC, less 1-octene will be needed, compared to 1-hexene, in order to achieve the same degree of disorganization of the crystalline phase (Figs. 1b, 2 and 3). Fig. 1b shows that only 7 mol% of 1-octene was required to completely destroy the copolymer crystallinity, whereas 21 mol% of 1-hexene was necessary to obtain the same result.

The decline in crystallization enthalpy and temperature cannot be attributed to the lower molecular weight of PHC compared to the homopolymer (Sample PP1) (values in Table 1), since homopolymer PP2 and all PHC have basically the same molecular weights. The concentration of short chain branches seems to be the main reason affecting the organization of the crystalline phase, which is supported by the fact that the longer the branch, the easier is the destruction of the crystalline structure.

Mülhaupt et al. [32] have studied the crystallization of metallocene syndiotactic poly(propylene-*co*-octene) and have concluded by X-ray diffraction measurements that the short chain branches are excluded from sPP crystals, following Flory's exclusion model [32–35]. Although it was not the purpose of this work to make an in-depth investigation of the copolymers crystalline morphology, it is quite reasonable to expect a similar behavior for metallocene isotactic poly(propylene-*co*-octene) and poly(propylene-*co*-hexene). That would also be in good agreement with what has been observed by several authors for ethylene/α-olefin copolymers, where alkyl branches larger than methyl are excluded from the polyethylene crystal lattice [36–38].

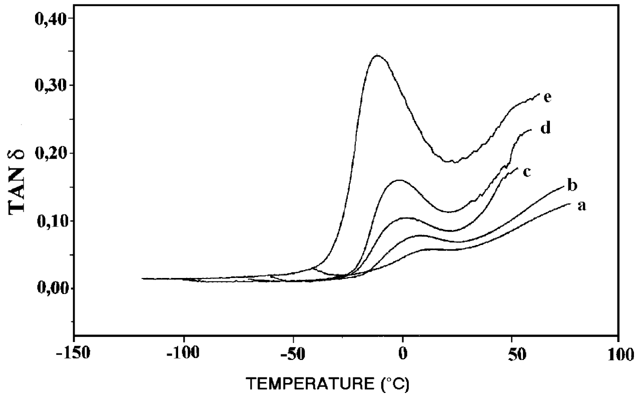

Fig. 4. Tan $\delta \times$ temperature plots for propylene copolymers with increasing 1-hexene contents: (a) [1-hexene] = 0.0, (b) 6.6, (c) 9.9, (d) 15.7, (e) 20.7 mol%.

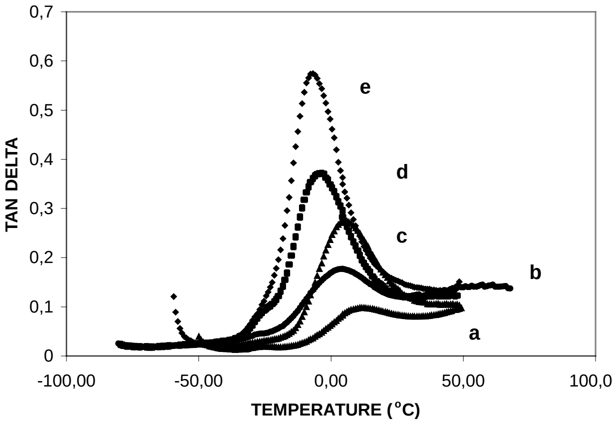

Fig. 5. Tan $\delta \times$ temperature plots for propylene copolymers with increasing amounts of 1-octene: (a) [1-octene] = 2.0, (b) 5.9, (c) 7.8, (d) 9.9, (e) 16.5 mol%.

Figs. 4 and 5 show the variation of tan δ with temperature for different PHC and POC, respectively. It can be observed that for incremental comonomer contents, there is a significant rise in the tan δ maxima values. Also the temperatures where the maxima of tan δ occurs, which are related to the glass transition temperatures (T_g), shift to lower values for higher amounts of comonomer in the copolymer. Again a straight correlation can be established between comonomer content and tan δ at the T_g (Fig. 6). These results are in very good accordance with what has been observed by Starck et al. [9,10] in their studies on ethylene/higher α-olefin copolymers.

A linear relationship is also observed between comonomer content in the copolymer and the storage modulus at room temperature (elastic modulus (E') at 25°C) (Fig. 7). This information gives a good indication about the copolymers stiffness and their performance in stress, hardness and impact tests at room temperature.

Another very good relationship was observed between T_g determined by DMTA at the maxima of the tan δ curves and comonomer content (Fig. 8). In a recent paper, Mülhaupt and coworkers [11] have presented a similar dependence between T_g and the concentration of short chain branches for metallocene ethylene/α-olefin copolymers and highly branched polyethylene prepared by Pd catalysts.

The influence of the short branch length is remarkable. Figs. 7–9 superposes the curves for the PHC and for POC, making it evident that much less 1-octene is necessary to

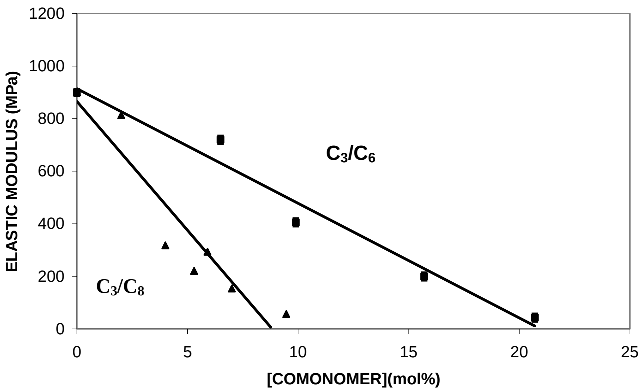

Fig. 6. Influence of comonomer concentration on the elastic modulus at 25°C for (■) propylene/1-hexene copolymers (PHC) (▲) propylene/1-octene copolymers (POC).

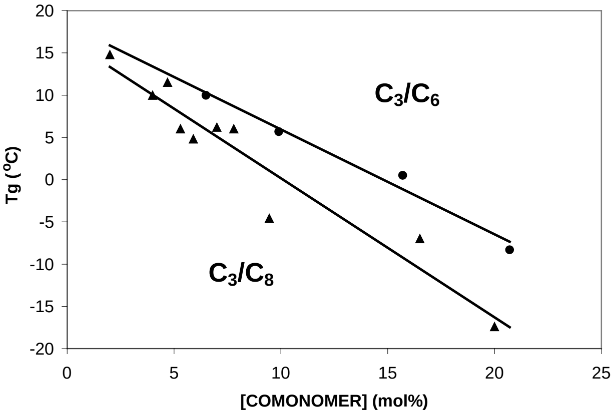

Fig. 8. Influence of comonomer type and content on the glass transition temperature (T_g): (▲) propylene/1-octene copolymers (POC); (●) propylene/1-hexene copolymers (PHC).

lower the T_g and impart rubbery behavior to the material. This is quite comprehensible, since the longer the alkyl branch, the farther apart will be the chains from each other and the more difficult it will be to organize the chains into lamellae and spherulites. So, this gain in mobility and flexibility will be sensed as a lowering of the glass transition temperature and storage modulus in DMTA measurements and in this case, as a decay of $T_{1\rho}^{\mathrm{H}}$ obtained by solid state ^{13}C NMR experiments (Tables 1 and 2).

Therefore, DMTA seems to be a very useful tool to predict mechanical properties of propylene copolymers based on these correlations between properties and chemical composition [39].

Since density is a very important property for the manufacturer, it was also investigated and once again a linear correlation between comonomer content and density was verified (Fig. 10). It can be observed from Fig. 10 that the incorporation of 1-hexene or 1-octene lowered the density of the copolymers. The short branches keep the polymer chains apart, creating more space between chains, which in a microscopic scale means a larger free volume and a reduction of crystallites size and in a macroscale will be translated into lower densities. The effect of the longer alkyl branch can be easily detected by a much sharper decline in density for the POC. A similar behavior has been observed by Yoon et al. [40] in their studies on metallocene ethylene/higher α-olefin copolymers.

It is known that solid state NMR provides a way to study the molecular dynamics down to a molecular size scale [29,41–43]. So, it was employed to evaluate molecular motion and materials' flexibility in order to establish a correlation with the information supplied by DMTA and the other characterization techniques used in this work. To our knowledge, there is no previous solid state NMR (Fig. 11) characterization of these metallocene propylene copolymers.

Fig. 12 shows the ^{13}C CPMAS NMR spectra for polypropylene and PHC and POC. The three major lines assigned in the spectra correspond to the CH_2 (44.5 ppm), CH (26.4 ppm) and CH_3 (21.8 ppm) groups of polypropylene.

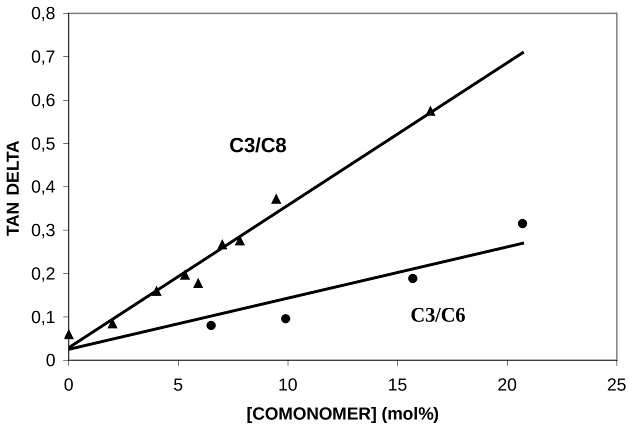

Fig. 7. Dependence of tan δ values (at T_g) on comonomer type and concentration: (▲) propylene/1-octene copolymers (POC); (●) propylene/1-hexene copolymers (PHC).

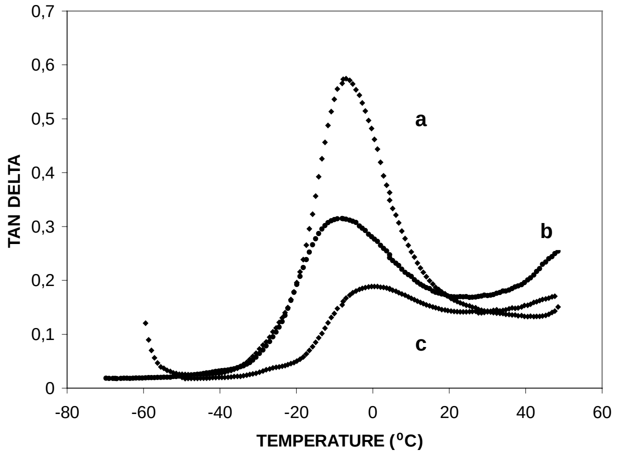

Fig. 9. Superposed tan δ × temperature plots for propylene copolymers: (a) [octene] = 16.5 mol%, (b) [hexene] = 20.7 mol%, (c) [1-hexene] = 15.7 mol%.

Table 2
$T_{1\rho}^{H}$ values for metallocene propylene/higher α-olefins copolymers

Sample	Comonomer	$T_{1\rho}^{H}$ (ms)		
		44.5 ppm[a]	26.4 ppm[a]	21.8 ppm[a]
PP1	None	27.0	27.2	26.1
PHC7	Hexene	21.5	21.6	21.0
PHC10	Hexene	17.9	18.0	17.0
PHC16	Hexene	16.7	16.9	16.6
PHC21	Hexene	15.3	15.5	14.9
POC4	Octene	23.8	23.7	22.6
POC7	Octene	11.0	10.5	9.8
POC17	Octene	8.7	7.9	6.6

[a] CH_2 (44.5 ppm), CH (26.4 ppm) and CH_3 (21.8 ppm) of polypropylene (see Fig. 12).

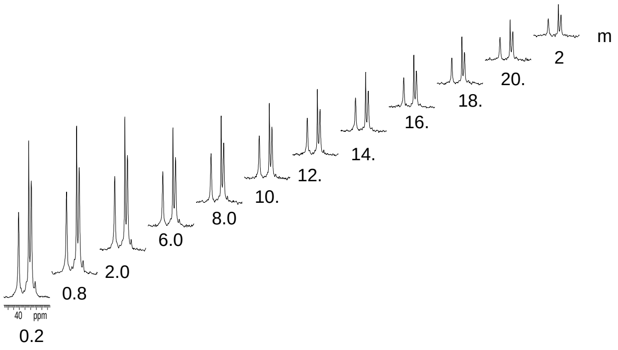

Fig. 11. Variable ^{13}C NMR signal intensity as a function of $^{1}H/^{13}C$ cross-polarization contact time of propylene/1-hexene copolymer ([1-hexene] = 20.7 mol%).

The additional 30.8 and 15.0 ppm lines belong to the CH_2 branches and CH_3 end groups from comonomers, respectively. The ^{13}C line shapes of the copolymers are similar to those of the corresponding homopolymer for the experimental conditions used in this work.

The CP/MAS NMR method [29,41–43] was employed to measure individual $T_{1\rho}$s for protons attached to different kinds of carbons. Proton $T_{1\rho}$ relaxation can be characterized by means of matched spin-locked, cross-polarization transfer experiments in which the carbon signal tracks the proton polarization as a function of proton high field decoupler contact time and thus follows its decrease via a $T_{1\rho}$ process (Fig. 11). This relaxation time is sensitive to motion at low frequency and was used to characterize differences in motion between the propylene copolymers presented in Table 2. However, it is first necessary to understand the dynamics of spin diffusion between polypropylene and copolymer protons. Table 2 displays $T_{1\rho}$ relaxations as detected by the protonated main chain carbons of high molecular weight polypropylene, PHC and POC. To measure $T_{1\rho}^{H}$ in these polymers, the sharper lines in the spectra have been monitored. Those are not pure lines and correspond to the crystalline structures under the influence of the amorphous phases [42,43]. Since $T_{1\rho}^{H}$ passes through a minimum as the samples correlation time varies, the relaxation behavior in these systems was modeled assuming the correlation time of the highly crystalline polypropylene to be at the lower frequency limit. So, changes in this parameter for the copolymer samples, in comparison to the PP relaxations, were discussed. It can be observed that for the same material, the carbons experiment slightly different $T_{1\rho}^{H}$ values. On the other hand, for copolymers with increasing comonomer content, $T_{1\rho}^{H}$ decreases, which, in this case, is indicating a gain in mobility. This increase in mobility can be attributed to a combination of two main effects, i.e. the reduction of the crystallite size and the greater mobility of the non-crystalline chains. Values for all $T_{1\rho}^{H}$s are reported in Table 2. For both systems, lower $T_{1\rho}^{H}$ values were observed for higher comonomer content and longer alkyl branch, indicating an

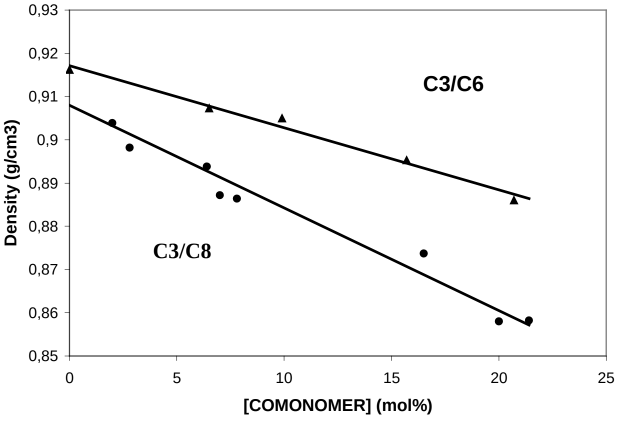

Fig. 10. Dependence of density on comonomer type and content: (▲) propylene/1-octene copolymers (POC); (●) propylene/1-hexene copolymers (PHC).

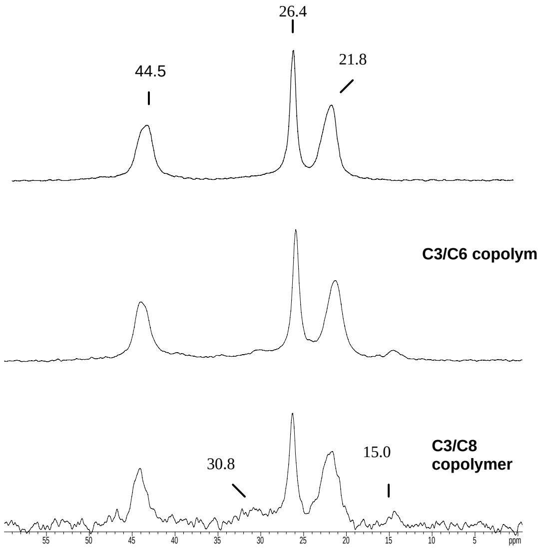

Fig. 12. CPMAS ^{13}C NMR spectra of polypropylene homopolymer, propylene/1-hexene copolymer ([1-hexene] = 20.7 mol%) and propylene/1-octene copolymer ([octene] = 16.5 mol%).

increase in the copolymer's flexibility. This result is corroborated by the T_g and tan δ measurements.

4. Conclusions

DSC and DMTA techniques have proved to be very useful techniques to establish correlations between the degree of comonomer incorporation in propylene copolymers and their thermal and mechanical properties. It was observed in this study that properties such as enthalpy of crystallization (ΔH_c), crystallization temperature (T_c), melting temperature (T_m), glass transition temperature (T_g), dynamic storage modulus (elastic modulus — E') and density decreased in a linear manner with increasing comonomer content in the copolymer.

That might allow to suggest the use of DSC, DMTA and density measurement, as fast and low cost analytical methods to determine comonomer content in propylene copolymers, in the studied range of concentration, as a less expensive alternative to solution state ^{13}C NMR. Of course, some prior information is required in order to develop a reliable analytical method, such as the type of comonomer that is incorporated in the copolymer, the concentration of stereo and regio defects in the chain (which is determined by the type of catalyst used and reaction conditions), the copolymers thermal history and a calibration curve, which must have been previously constructed with standards of known comonomer concentration, determined by solution ^{13}CNMR.

Solid state ^{13}C NMR showed excellent correlation with the results obtained by DMTA. Lower $T_{1\rho}^{H}$ values were observed for higher comonomer content and longer alkyl branch, which, in this case, indicate an increase in copolymers' flexibility. That finds correspondence to the lowering of storage modulus, the decline in glass transition temperature (T_g) and the increase of tan δ in DMTA experiments.

The effect of the short branch length is quite noteworthy and affects all measured properties. It was observed that the longer the alkyl branch, the less comonomer was necessary to separate the polymer chains and disrupt the crystalline structure. It, therefore, increases the free volume and the amorphous phase and reduces the size of crystallites, which will be translated into lower densities and rubbery behavior of the copolymers.

Based on the structure–property relationships herein described, one can infer about these copolymers impact resistance and other important end-use properties.

Acknowledgements

The authors would like to thank CNPq, PRONEX, PADCT/CNPq, FAPERJ and Polibrasil Resinas S.A for the financial support and Witco GmbH for MAO donation.

References

[1] Hlatky GG. Coord Chem Rev 2000;199:235–329.
[2] Hlatky GG. Coord Chem Rev 1999;181:243–96.
[3] Kamisnsky W. J Chem Soc, Dalton Trans 1998;9:1413–8.
[4] Kamisnsky W, Arndt M. Adv Polym Sci 1997;127:143–87.
[5] Moore EP. Polypropylene handbook. Munich: Hanser Publishers, 1996, p. 403–9.
[6] Krentsel BA, Kissin YV, Kleiner VI, Stotskaya LL. Polymers and copolymers of higher α-olefins. Chemistry, technology, applications. Munich: Hanser Publishers, 1997 (Chapter 8).
[7] Simanke AG, Galland GB, Freitas L, Jornada JAH, Quijada R, Mauller RS. Polymer 1999;40:5489–95.
[8] Lehtinen C, Starck P, Löfgren B. J Polym Sci, Part A: Polym Chem 1997;35:307–18.
[9] Starck P. Eur Polym J 1997;33(3):339–48.
[10] Starck P, Lehtinen C, Löfgren B. Angew Makromol Chem 1997; 249:115–35.
[11] Mäder D, Heinemann J, Walter P, Müllhaupt R. Macromolecules 2000;33:1254–61.
[12] Lovisi H, Marins E, Tiziano G, Menezes SMC, Santa Maria LC, Coutinho FMB. Proceedings of Advances in Polyolefins II, Napa, CA, USA, 1999.
[13] Cho CJH, Soares JBP, Tzoganakis C. Proceedings of ANTEC 2000, Houston, TX, 2000. p. 1663–6.
[14] Tincul I, Joubert DJ. Polypropylene '99 — 8th Annual World Congress, Switzerland, 1999.
[15] Tritto I, Donetti R, Sacchi MC, Locatelli P, Zanoni G. Macromolecules 1999;32:264–9.
[16] Forlini F, Fan ZQ, Tritto I, Locatelli P, Sacchi MC. Macromol Chem Phys 1997;198:2397–408.
[17] Kim I, Kim YJ. Polym Bull 1998;40:415–21.
[18] Kim I. Macromol Rapid Commun 1998;19:299–303.
[19] Jungling S, Koltzemburg S, Mülhaupt R. J Polym Sci, Part A: Polym Chem 1997;35:1–8.
[20] Beck S, Brintzinger HH, Suhm J, Mülhaupt R. Macromol Rapid Commun 1998;19:235–9.
[21] McAlpin JJ, Stahl GA. Proceedings of MetCon'94, Houston, TX, USA, 1994.
[22] Yang SL, Xu ZK, Feng LX. Makromol Chem Macromol Symp 1992;63:233–43.
[23] Xu ZK, Feng LX, Wang D, Yang SL. Makromol Chem 1992; 192:1835–40.
[24] Arnold M, Henschke O, Knorr J. Macromol Chem Phys 1996; 197:563.
[25] Krentsel BA, Kissin YV, Kleiner VI, Stotskaya LL. Polymers and copolymers of higher α-olefins. Chemistry, technology, applications. Munich: Hanser Publishers, 1997. Chapter 4, p. 103–7.
[26] Dariva C, Lovisi H, Santa Maria LC, Coutinho FMB, Pinto JC, Oliveira JW. Canadian Journal of Chemical Engineering 2001, submitted for publication.
[27] Density and specific gravity (relative density) of plastics by displacement. ASTM D 792-91, Section 8, vol. 08.01. Philadelphia, PA, USA: ASTM, 1994. p. 185–8.
[28] Cheng HN. Polym Commun 1984;25:99–105.
[29] Shin ID, Zhang S, Stejskal EO. J Magn Reson, Ser A 1994;109:192–7.
[30] Busico V, Cipullo R, Caporaso L, Angelini G, Segre A. J Mol Catal Chem 1998;128:53–64.
[31] Unpublished results.
[32] Thomann R, Kressler J, Mülhaupt R. Polymer 1998;39(10):1907–15.
[33] Flory PJ. Trans Faraday Soc 1955;51:848.
[34] Cheng SZD, Janimak JJ, Zhang A. Polymer 1991;32(4):648–55.
[35] Crist B, Mirabella FM. J Polym Sci, Part B: Polym Phys 1999; 37:3131–40.
[36] Alamo RG, Mandelkern L. Thermochim Acta 1994;238:155.
[37] Androsch R. Polymer 1999;40:2805–12.

[38] Cerrada ML, Benavente R, Peña B, Pérez E. Polymer 2000;41:5957–65.
[39] Sepe MP. Dynamic mechanical analysis for plastics engineers. Norwich, NY: Plastics Design Library, 1998.
[40] Yoon JS, Lee DH, Park ES, Lee IM, Park DK, Jung SO. Polymer 2000;41:4523–30.
[41] Silva NM, Tavares MIB, Stejskal EO. Macromolecules 2000;33:115–9.
[42] VanderHart DL, Alamo RG, Nyden MR, Kim MH, Mandelkern L. Macromolecules 2000;33:6078–93.
[43] Alamo RG, VanderHart DL, Nyden MR, Mandelkern L. Macromolecules 2000;33:6094–105.